

Impact of mountain pine beetle outbreaks on forest albedo and radiative forcing, as derived from Moderate Resolution Imaging Spectroradiometer, Rocky Mountains, USA

M. Vanderhoof,¹ C. A. Williams,¹ B. Ghimire,^{1,2} and J. Rogan¹

Received 17 May 2013; revised 4 September 2013; accepted 19 September 2013.

[1] Mountain pine beetle (*Dendroctonus ponderosae*) outbreaks in North America are widespread and have potentially large-scale impacts on albedo and associated radiative forcing. Mountain pine beetle outbreaks in Colorado and southern Wyoming have resulted in persistent and significant increases in both winter albedo (change peaked 10 years post outbreak at 0.06 ± 0.01 and 0.05 ± 0.01 , in lodgepole pine (*Pinus contorta*) and ponderosa pine (*Pinus ponderosa*) stands, respectively) and spring albedo (change peaked 10 years post outbreak at 0.06 ± 0.01 and 0.04 ± 0.01 , in lodgepole pine and ponderosa pine stands, respectively). Instantaneous top-of-atmosphere radiative forcing peaked for both lodgepole pine and ponderosa pine stands in winter at 10 years post outbreak at $-1.7 \pm 0.2 \text{ W m}^{-2}$ and $-1.4 \pm 0.2 \text{ W m}^{-2}$, respectively. The persistent increase in albedo with time since mountain pine beetle disturbance combined with the continued progression of the attack across the landscape from 1994–2011 resulted in an exponential increase in winter and annual radiative cooling (MW) over time. In 2011 the rate of radiative forcing within the study area reached $-982.7 \pm 139.0 \text{ MW}$, $-269.8 \pm 38.2 \text{ MW}$, $-31.1 \pm 4.4 \text{ MW}$, and $-147.8 \pm 20.9 \text{ MW}$ in winter, spring, summer, and fall, respectively. An increase in radiative cooling has the potential to decrease sensible and/or latent heat flux by reducing available energy. Such changes could affect current mountain pine beetle outbreaks which are influenced by climatic conditions.

Citation: Vanderhoof, M., C. A. Williams, B. Ghimire, and J. Rogan (2013), Impact of mountain pine beetle outbreaks on forest albedo and radiative forcing, as derived from Moderate Resolution Imaging Spectroradiometer, Rocky Mountains, USA, *J. Geophys. Res. Biogeosci.*, 118, doi:10.1002/jgrg.20120.

1. Introduction

[2] Current outbreaks of bark beetles (Coleoptera: Curculionidae, Scolytinae) in western North America are some of the largest and most severe in recorded history [Bentz et al., 2009]. Since 1997, more than 41.7 million acres have been affected by bark beetles in the western United States and more than 6.6 million acres in Colorado alone [USDA Forest Service, 2011]. During an attack the needles of a host tree typically turn red within 12 months (red attack stage) and fall off within 3 years (gray attack stage) [Mitchell and Preisler, 1998]. Snags begin to fall 5 years after stand death, with blow down peaking after 10–15 years [Mitchell and Preisler, 1998; Huggard and Lewis, 2007]. In recent years (1996 to present) Colorado outbreaks of mountain pine

beetles (*Dendroctonus ponderosae*) have reduced the live basal area of lodgepole pine (*Pinus contorta*) dominated forests by 70%, on average [Klutsch et al., 2009]. The current extent and high severity (percent tree mortality) of these recent mountain pine beetle outbreaks has been attributed to warmer summer and winter temperatures and drought conditions associated with regional climate change [Berg et al., 2006; Raffa et al., 2008]. Warming and reduced precipitation trends have increased over winter survival of beetle populations, increased the rate of reproduction and maturation, and created drought-induced stress in tree hosts [Berg et al., 2006; Raffa et al., 2008].

[3] Mountain pine beetle outbreaks result in tree mortality, temporarily reducing live tree density and changing stand albedo. Multiple studies have documented a significant increase in annual albedo with forest loss or disturbance due to the increased exposure of white snow during winter months instead of dark vegetation from above the canopy [Betts, 2000; Bala et al., 2007]. A change in albedo due to a forest disturbance event modifies the amount of shortwave radiation absorbed at the surface as well as the amount of longwave radiation absorbed and emitted at the surface [Zhang et al., 1995]. This change in radiation or energy is imposed on the climate system as a direct climate forcing

¹Graduate School of Geography, Clark University, Worcester, Massachusetts, USA.

²Lawrence Berkeley National Laboratory, Berkeley, California, USA.

Corresponding author: M. Vanderhoof, Graduate School of Geography, Clark University, 950 Main Street, Worcester, MA 01610, USA. (mevanderhoof@clarku.edu)

and is typically reported as a change in energy flux at the top of the tropopause, otherwise referred to as top-of-atmosphere. Top-of-atmosphere radiative forcings are useful as they are closely related to global mean surface temperature for a wide range of forcing agents [Hansen *et al.*, 1997; Committee on Radiative Forcing Effects on Climate, 2005]. In addition to potential changes in albedo, mountain pine beetle outbreaks also cause an increase in CO₂ emissions, resulting from the decomposition of killed trees. Although these CO₂ emissions result in a direct climate response, the albedo effect has been found to outweigh the CO₂ climate response in boreal and high-elevation regions [Betts, 2000; Randerson *et al.*, 2006; Bala *et al.*, 2007]. In addition to the direct radiative forcings caused by CO₂ emissions and albedo, reductions in vegetation as well as albedo-driven changes in net radiation can result in indirect radiative forcings caused by altered cloud cover, evapotranspiration, and sublimation. Recent studies have shown a decrease in summer evapotranspiration at regional and watershed scales following bark beetle outbreaks [Mikkelsen *et al.*, 2013; Maness *et al.*, 2013], which could have implications on regional cloudiness and precipitation patterns [Bala *et al.*, 2007].

[4] Despite wide recognition of the large extent and severity of recent mountain pine beetle outbreaks, an assessment of landscape- and regional-scale impacts on albedo is still lacking. Studies focused at the site scale have documented a below-canopy decrease in winter albedo 1–3 years post attack due to needle and litter accumulation on snow [Winkler *et al.*, 2010; Pugh and Small, 2012] and a significant increase in winter, but not summer, albedo post red attack stage (>3 years post attack) [O'Halloran *et al.*, 2012]. Studies to date, however, fail to document if site-based changes persist at landscape scales (hundreds of kilometers squared) and focus almost exclusively on lodgepole pine stands, ignoring potential differences between stand types [Winkler *et al.*, 2010]. This study explores (1) the seasonal change in albedo with time since mountain pine beetle attack and forest type and (2) how a growing area of outbreak drives landscape-scale radiative forcing. The temporal lag in needle loss, snag fall, and forest regrowth coupled with an annually expanding area of attacked forest implies a prolonged impact on forest structure, albedo, and potential climate.

2. Methods

[5] In this study mountain pine beetle outbreak polygon data (1994–2011) were related to Moderate Resolution Imaging Spectroradiometer (MODIS) albedo data (MCD43A3) (2000–2011). Combining sites with the same number of years since the start of the attack, we derived characteristic curves describing the change in albedo with time since the attack started for lodgepole pine and ponderosa pine (*Pinus ponderosa*) forests within Colorado and southern Wyoming. Change in albedo was translated into radiative forcing to calculate the albedo-driven climate forcing effect of outbreaks on coniferous forests.

2.1. Study Area

[6] The study area included all lodgepole pine and ponderosa pine dominated forests within Colorado and southern Wyoming, as classified by the U.S. Department of Agriculture (USDA) Forest Service, Forest Inventory and Analysis

(FIA) Program data (250 m resolution) [Ruefenacht *et al.*, 2008]. Lodgepole pine and ponderosa pine forests within southern Wyoming were included so that the study area was defined using natural topographic boundaries (i.e., forest extent) and not artificial boundaries (i.e., state border). Lodgepole pine and ponderosa pine forests are typically found on the lower slopes and valleys above the foothills at elevations between 2100 and 2900 m above sea level. Stands dominated by the two host tree species, lodgepole pine and ponderosa pine, were analyzed separately to account for species-specific differences in damage patterns and forest structure. Both of these forest types represent an important forest cover type within the region. Within the study area (Colorado and southern Wyoming), forests classified as lodgepole pine and ponderosa pine each cover ~1.2 million ha. The combined lodgepole pine and ponderosa pine forest extent within Colorado alone (~2.2 million ha) corresponds to approximately 8% of the state's land area. Based on climatological records from Estes Park, CO (2365 m elevation), mean annual precipitation is 540 mm, while the average low and high temperature are −9°C in January and 25°C in July, respectively. Topography and thus microclimate vary substantially within the study area.

2.2. Data

[7] Mountain pine beetle damage data were provided by U.S. Forest Service, Region 2 Aerial Detection Survey Data (USFS ADS) (1994–2011). Expert surveyors document areas of new mountain pine beetle damage by drawing polygons around the affected area(s) observed during aerial field surveys. Although ADS surveys typically overestimate the area damaged (B. Howell, USFS, personal communication, 2012), they are currently the most comprehensive source of mountain pine beetle damage available in the U.S. The year in which an attack began for a given location was specified as the first survey year in which a site was recorded within a mountain pine beetle damaged polygon. Because more limited areas were flown in the early years of the surveys (1994–2000) relative to more recent years (2001–2011), a fraction of outbreaks may have experienced delayed reporting of the date when the attack started. To partially compensate for this potential source of error, survey information for 1994–1997 was combined. This decision was also due to the minimal area of damage recorded for each of these years (<20,000 ha per year) relative to later years (39,000 to 183,000 ha per year).

[8] Albedo was derived from the Moderate Resolution Imaging Spectroradiometer (MODIS) Collection 5 BRDF/Albedo 16 day 500 m product (MCD43A3), which couples a semiempirical, RossThick-LiSparse kernel-driven bidirectional reflectance distribution function (BRDF) model with multi-date, cloud-free, atmospherically corrected surface reflectance to determine the anisotropy of global land surfaces at a 500 m spatial resolution [Schaaf *et al.*, 2002]. Steep topography, as is observed in the south-central Rocky Mountains, can affect both the viewing zenith angle and solar zenith angle, which in turn has the potential to bias albedo values [Jin *et al.*, 2003; Painter *et al.*, 2009]. To minimize such bias, broadband white-sky albedo was used as it is independent of view and solar angle and thus albedo can be compared across a heterogeneous space (e.g., mountainous region) and time (e.g., months and years) [Gao *et al.*, 2005]. This approach of using white-sky albedo to quantify changes in land cover or land condition

has been used by others in similar work [Barnes and Roy, 2008, 2010; Maness et al., 2013]. To capture seasonal and interannual albedo variation, 12 dates (midmonth) (day of year: 017, 041, 073, 105, 137, 169, 201, 225, 257, 289, 321, and 353) were used for all of the 12 available years (2000–2011) of shortwave (0.3–5.0 μm) broadband white-sky albedo data (total of 144 scene dates). We rejected all observations with cloud cover, bad quality, or fill values based on data quality flags. Near-infrared broadband white sky was also tested, but similarity in findings to shortwave broadband white sky led to its exclusion. The accuracy of the MODIS Collection 5 shortwave albedo is reported as 0.05 but is generally <0.03 [Roman et al., 2009; Wang et al., 2010].

[9] Although not incorporated into the analysis, field-collected tree plot data were used to support methodological decisions and help explain the findings. In lodgepole pine and ponderosa pine dominated stands, 55 and 53 tree plots were collected, respectively, from 18 June to 20 July 2012, within 900 m^2 plots (97,200 m^2 total). These plots were located in Roosevelt National Forest, Rocky Mountain National Park, and Arapaho National Forest within Colorado. Plots were targeted to be representative of (1) the surrounding 500 m \times 500 m area, (2) a severity spectrum (from none to severe) of bark beetle outbreak, and (3) a spectrum of time since attack (green attack, red attack, and gray attack stages). Within each plot, each tree was identified to the species level, its diameter measured (diameter at breast height (DBH) >7.5 cm) and recorded as unattacked (no evidence of beetle presence), green attack stage (exit holes and pitch tubes present but needles still green), red attack stage (exit holes and pitch tubes present and needles red), gray attack stage (exit holes and pitch tubes present and needles absent), or unknown dead (needles absent but no evidence of beetle damage). Sapling and seedling (DBH <7.5 cm) abundance and species composition were sampled in two 25 m^2 subplots within each plot. Mean canopy height was measured using a clinometer, canopy cover was measured using a densitometer, and understory cover (vegetation, litter, and bare rock) was visually estimated.

2.3. Analysis

[10] In addition to the data preparation steps mentioned above, several steps were taken to minimize mixed pixels and reduce problems of scale between data sets. First, an internal buffer of 500 m was applied to lodgepole pine and ponderosa pine forest extent, as defined by the FIA data set, to increase confidence regarding forest type. All fire scars (1984–2011), derived from Monitoring Trends in Burn Severity (MTBS) data, were masked out [Eidenshink et al., 2007]. All available years of fire scars were used, including fire scars up to 10 years prior to the start of mountain pine beetle data, to account for lasting albedo effects from past fires. In addition, to reduce the inclusion of mixed pixels (damaged and nondamaged forest) and to reduce problems of scale between the MODIS albedo data and the ADS data, only mountain pine beetle damaged locations derived from polygons larger than 30 ha were included in the analysis. As a single-albedo pixel is 25 ha, if small infestation polygons (i.e., less than 25 ha) were used, it is likely that the albedo effect would have been diluted due to the albedo pixel representing both attacked and non-attacked forest. The threshold of 25 ha was increased 30 ha to account for spatial mismatches between polygon boundaries and albedo pixel boundaries.

[11] Unlike a fire or storm event, a mountain pine beetle outbreak progresses spatially over multiple years. Each MODIS scene contained pixels that experienced mountain pine beetle damage 1 to n years ago, as well as sites that were 1 to n years from being attacked. For each month (image date), pixels across scene years (2000–2011) were grouped based on the number of years since the attack started; thus, each group was uniform with regard to time since mountain pine beetle attack but was comprised of pixels from different scene years. Because albedo values from multiple years were used, we needed to consider potential sources of error due to interannual variability. Interannual variability in MODIS albedo can be due to (1) inherent differences in stand density, structure, snow cover, and data quality between pixels for each group, from each scene year, and (2) phenological differences due to interannual climate variability [Gao et al., 2005]. Variation due to inherent differences in input pixels was minimized by setting minimum sample sizes and by filtering input data sets (FIA and ADS) as described both above and in section 2.2. Variation due to interannual climate variability was minimized by normalizing data, so that each pixel was calculated as the change in albedo from the within-scene non-attacked lodgepole pine or ponderosa pine forest, respectively. As non-attacked forests may have experienced changes in albedo due to harvest activities, small fires undocumented by the MTBS data set, human development, or other unmapped sources of disturbance, non-attacked forest was defined as forest that was 2 years from being classified as “attacked” by ADS data. One year prior to disturbance was not used due to the potential effect of mountain pine beetle outbreak’s green stage (trees are attacked, but needles are not yet red). Thus, non-attacked forest was comparable (with regard to stand density and structure) to the forests attacked by mountain pine beetle, prior to their attack. Both snow and snow-free pixels were included in order to capture seasonal changes in snow cover. Each group of pixels was then averaged to derive mean change in albedo (for each month) with time since the attack started for lodgepole pine and ponderosa pine forests.

[12] Using the above approach, we were unfortunately unable to quantify change in albedo based on outbreak severity. The severity of outbreaks (and corresponding change in albedo) naturally varies across the landscape but was not explicitly included in the analysis due to a lack of accurate severity data. When the USFS ADS severity data were compared to our field-collected tree plot data, we found the USFS estimated mean tree mortality (24 ± 2 and 29 ± 2 trees killed per acre for lodgepole pine and ponderosa pine plots, respectively) to be underestimated by a factor of 16 ± 4 and 6 ± 1 trees per acre for lodgepole pine and ponderosa pine stands, respectively. By not explicitly including severity data in the analysis, the mean change in albedo resulting from mountain pine beetle outbreak was seen as representative of the region’s mean severity of outbreak (mean percent tree mortality). Klutsch et al. [2009] quantified this mean severity as a 70% reduction in live basal area for lodgepole pine stands. Additionally, although our field plots were not selected randomly but rather to represent a range of severities (percent tree mortality) within mountain pine beetle damaged lodgepole pine stands, the percent of trees killed by beetles ranged from 6.5% to 88% with a mean percent mortality of $49 \pm 3\%$. Within mountain pine beetle damaged ponderosa

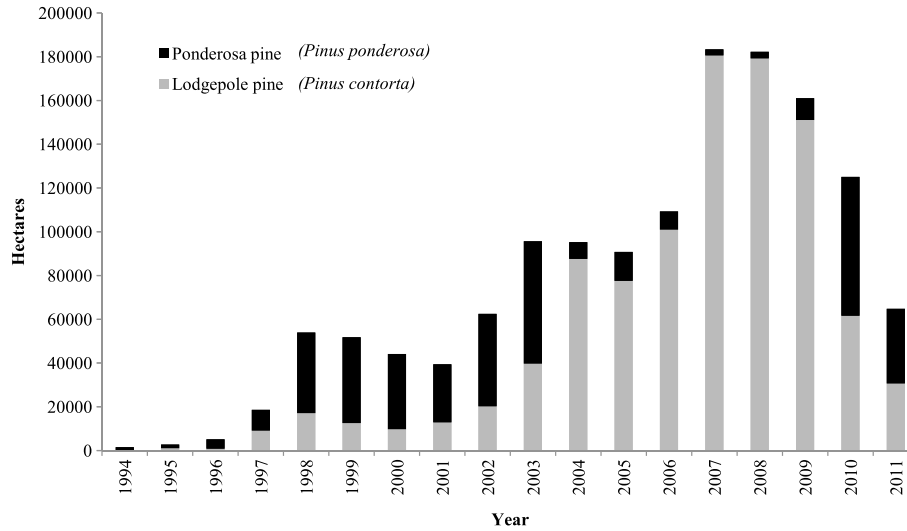


Figure 1. Total area (ha) designated as mountain pine beetle attacked by USFS ADS data, by forest type and year of attack (stacked bars), within Colorado and southern Wyoming.

pine plots, the percent mortality ranged from 20 to 90% with a mean percent mortality of $48 \pm 3\%$.

2.4. Radiative Forcing

[13] While surface radiative forcing is relevant for the surface energy balance, top-of-atmosphere radiative forcing was calculated, as recommended by the Intergovernmental Panel on Climate Change (IPCC), as it quantifies the true impact of the disturbance event on climate. Top-of-atmosphere forcing values can be expected to be a fraction of the surface forcing due to the attenuation of the upwelling beams by clouds and aerosols. The top-of-atmosphere radiative forcing was calculated using the radiative kernel technique, which represents changes to top-of-atmosphere radiative fluxes caused by changes in monthly average surface albedo, relative to non-attacked forest values at 2.5° resolution, which was resampled to 1° resolution to better match the spatial extent of the study area [Shell *et al.*, 2008]. The kernel (K) was produced using the offline radiative transfer model from the National Center for Atmospheric Research (NCAR) Community Atmospheric Model version 3 [Collins *et al.*, 2006] as described in Shell *et al.* [2008] and reported as the radiative forcing response to a 0.01 change in albedo, where

$$\Delta F_{\text{TOA}} = \Delta \alpha \cdot K^{\alpha} \quad (1)$$

where α is the shortwave albedo. Equation 1 was used to derive mean top-of-atmosphere radiative forcing by season, with years since the attack started. This technique was similarly used by O'Halloran *et al.* [2012] to calculate top-of-atmosphere radiative forcing for forest disturbance events. It is possible that the spatial mismatch between the kernel resolution and the MODIS albedo product could have resulted in a bias in our reported top-of-atmosphere radiative forcing estimates. As mountain pine beetle damage is concentrated in mountainous areas, kernels spanning both mountains and valley or plateau regions may have shown biased atmospheric properties because of the topographic effect on cloud cover. Although this is beyond the scope of the present work, future investigations could consider

the use of a regional climate model to more precisely characterize the radiative kernel.

[14] Top-of-atmosphere radiative forcing is referred to as radiative forcing in the remaining text. We interpreted radiative forcing in several additional ways: (1) radiative forcing was summed per year (MW) using the chronosequence curves applied to all beetle-affected pixels along with the maps of forest type (ponderosa pine or lodgepole pine) and years since outbreak, (2) the cumulative radiative forcing (1994–2011) was mapped across the study area (MJ m^{-2}), and (3) global radiative forcing was calculated by dividing the cumulative radiative forcing by the surface of the earth. We implemented a conservative assumption of nonrandom error propagation for which uncertainty was combined as the product of those for the MODIS albedo product and the radiative kernels. A 10% uncertainty was assumed for both the MODIS albedo product and the radiative kernels. This method of uncertainty propagation is analogous to an IPCC Tier 1 uncertainty [Intergovernmental Panel on Climate Change, 2000].

3. Results

[15] The total area attacked within lodgepole pine and ponderosa pine forests (1994–2011) represented 48% and 21%, respectively, of total forest area for each forest type within Colorado and southern Wyoming, respectively. Area of outbreak peaked in 2007 and 2008, with each year contributing 13% of the total outbreak area over the time period (1994–2011) (Figure 1). Two large jumps in the annual area of outbreak were observed, the first between 1997 and 1998 and the second between 2006 and 2007 (Figure 1). However, we were unable to correlate these two jumps in outbreak area with any multi-year patterns in precipitation or temperature, as derived from NOAA National Climatic Data Center, Division 2 data. During the outbreak period the mountain pine beetle outbreak alternated between occurring predominately in lodgepole pine and ponderosa pine stands. More than 50% of the outbreak area occurred within ponderosa pine stands during 1994–2003 (Figure 1).

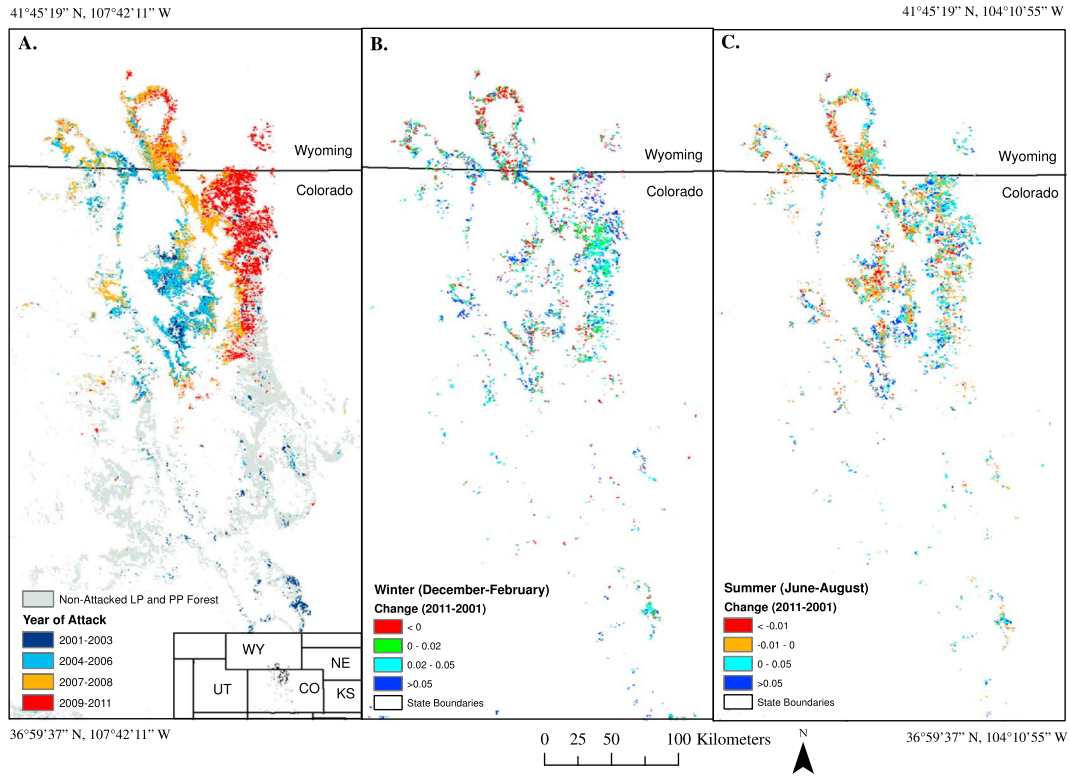


Figure 2. (a) Extent of mountain pine beetle damage (2001–2011) in lodgepole and ponderosa pine forests within Colorado and southern Wyoming. (b) Albedo change in winter within mountain pine beetle damaged areas, from 2001 to 2011. (c) Albedo change in summer within mountain pine beetle damaged areas, from 2001 to 2011.

From 2004 through 2009, meanwhile, lodgepole pine stands represented 85–98% of the outbreak area. In the last 2 years (2010–2011) the outbreak was approximately equally split between the two forest types. The recent decline in lodgepole pine outbreak area, observed in 2010 and 2011, relative to the previous several years may be due to an exhaustion of available host trees, as well as the renewed activity of the beetles within ponderosa pine forests.

[16] To look at the impact of these outbreaks on forest albedo, we first calculated a change in albedo across mountain

pine beetle attacked forest using a simple subtraction approach (2011 MODIS albedo – 2001 MODIS albedo) (Figure 2). Changes in albedo across this time period were not spatially uniform. Differences in albedo change can be attributed to multiple potential causes, including variation in the date when the attack started and the age of outbreak. Additional variability could be due to differences in outbreak severity, starting stand density, stand condition, or rate of stand recovery. Field work within selected areas showing a large increase in winter albedo confirmed that these areas experienced high

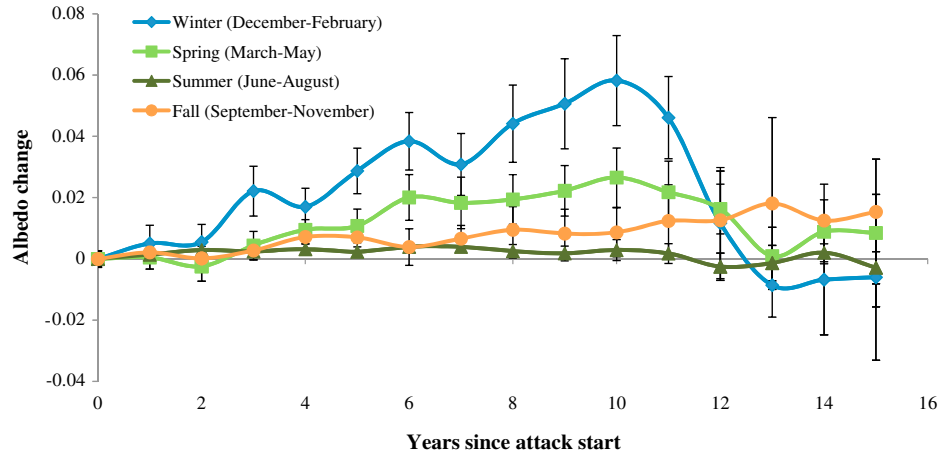


Figure 3. Mean change in white-sky albedo, by season, with time since the attack started in lodgepole pine stands. Error bars represent plus and minus standard error.

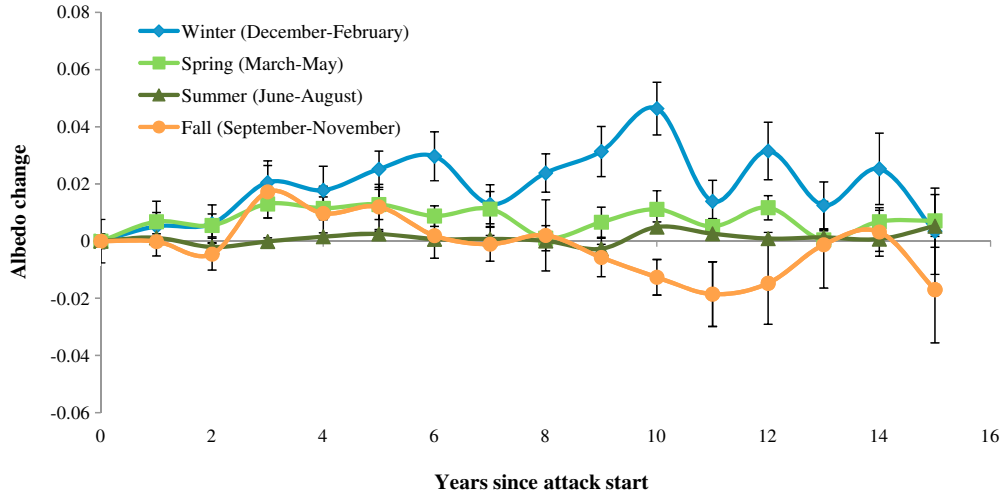


Figure 4. Mean change in white-sky albedo, by season, with time since the attack started in ponderosa pine stands. Error bars represent plus and minus standard error.

rates of tree mortality and snag fall. Other mountain pine beetle damaged areas, such as Medicine Bow National Forest (in the northernmost part of the study area), have experienced extensive logging and regrowth in addition to widespread mountain pine beetle outbreaks, which may explain the observed decline in albedo between 2001 and 2011 in some portions of the forest. This implies that logging activities, not currently mapped, could potentially influence landscape-scale findings. It must be noted, however, that this simple subtraction method is problematic as it (1) ignores change due to interannual variability between 2001 and 2011, (2) may not capture change in albedo for stands attacked prior to 2001, (3) may not capture change in albedo for rapidly revegetating sites, and (4) can only conduct analysis on pixels where data values are available for both dates. Therefore, although the curves developed in this study must be viewed as an average across the landscape, our approach,

as outlined in section 2.3, avoids the problems mentioned above by deriving change in albedo with time since the attack started using the entire 2001 to 2011 MODIS albedo series in a chronosequence approach.

[17] When monthly changes in albedo (using the chronosequence approach) were averaged by season, both lodgepole pine and ponderosa pine stands showed a consistent and significant increase in albedo in response to mountain pine beetle damage in winter (December–February) (lodgepole pine, 3–11 years and ponderosa pine, 3–10 years) and spring (March–May) (lodgepole pine, 4–12 years and ponderosa pine, 3–7, 10, 12, and 14 years) ($p < 0.05$) (Figures 3 and 4). Both forest types exhibited a multi-year lag effect before a significant change in winter albedo was seen 3 years post attack ($p < 0.05$). In lodgepole pine stands, change in winter albedo reached 0.02 ± 0.01 by 3 years post attack and increased linearly to a maximum of 0.06 ± 0.01 10 years

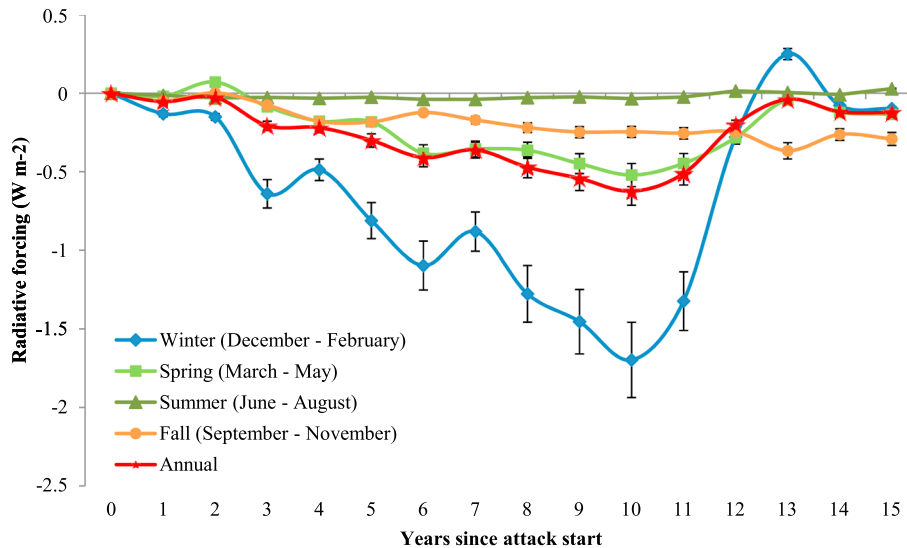


Figure 5. Mean instantaneous top-of-atmosphere radiative forcing (W m^{-2}), by season with time since the attack started in lodgepole pine stands. Error bars represent uncertainty as derived from within data set errors.

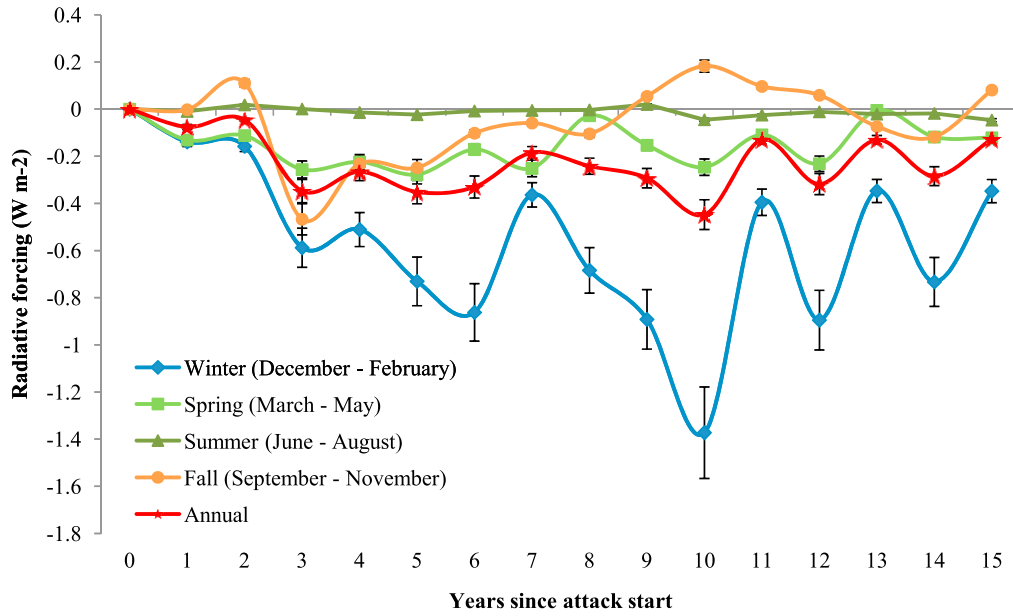


Figure 6. Mean instantaneous top-of-atmosphere radiative forcing (W m^{-2}), by season with time since the attack started in ponderosa pine stands. Error bars represent uncertainty as derived from within data set errors.

post attack (Figure 3). At a monthly timescale, change in albedo peaked in January 10 years post attack and in February 9 years post attack (0.07 ± 0.01 and 0.06 ± 0.001 , respectively). In ponderosa pine stands, change in winter albedo also reached 0.02 ± 0.01 by 3 years post attack but increased less linearly to a slightly lower maximum change of 0.05 ± 0.01 10 years post attack (Figure 4). At a monthly timescale, change in albedo peaked in January 10 years post attack and in December 10 and 14 years post attack (0.06 ± 0.01 , 0.05 ± 0.01 , and 0.05 ± 0.01 , respectively). In lodgepole pine and ponderosa pine stands, significant increases in spring albedo were largely driven by large observed increases in March albedo, which peaked 9–11 years post attack in lodgepole pine stands (0.05 ± 0.01 , 0.06 ± 0.01 , and 0.06 ± 0.01 , respectively) and 7 and 10 years post attack in ponderosa pine stands (0.04 ± 0.01 and 0.03 ± 0.01 , respectively).

[18] During the predominately snow-free season, both lodgepole pine and ponderosa pine stands showed a consistent increase in summer and fall albedos in response to mountain pine beetle outbreak (Figures 3 and 4), but this change was almost entirely either not significant or within the range of error inherent to the MODIS albedo product. Change to albedo was consistently closest to zero during the summer months for both lodgepole pine and ponderosa pine stands throughout the years since the attack, with the least amount of change observed during June for lodgepole pine stands and July for ponderosa pine stands. When we compared the response between lodgepole pine and ponderosa pine stands, seasonal patterns in albedo change were similar but lodgepole pine stands showed a significantly larger change in albedo for some years in the winter (years 7, 8, and 11 since the outbreak started) and spring (years 6, 8–11 since the outbreak started) seasons ($p < 0.05$).

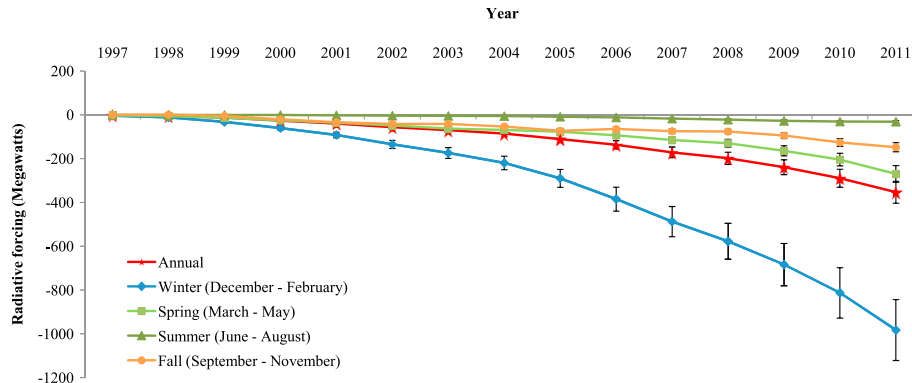


Figure 7. Per year top-of-atmosphere radiative forcing (MW) within the study area, as derived from accumulating area of attack and the distribution of years since the outbreak started. Forcing is cumulative within each year but not across the time period. Error bars represent uncertainty as derived from within data set errors.

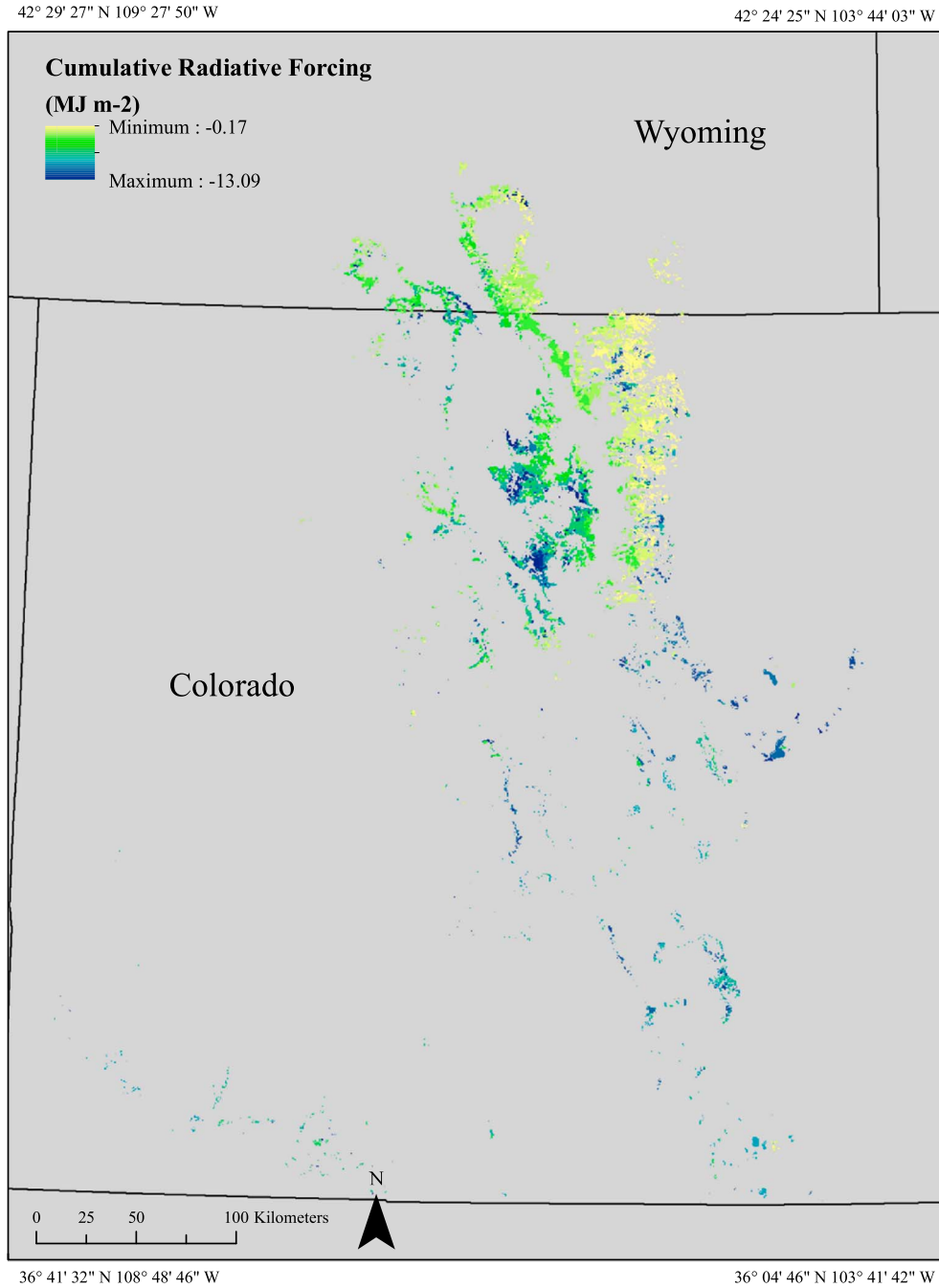


Figure 8. The spatial distribution of the cumulative (1994 to present) top-of-atmosphere radiative forcing (MJ m^{-2}) within mountain pine beetle attacked forest as derived from a monthly time step of change in albedo, forest type (lodgepole pine or ponderosa pine), and years since the outbreak started.

[19] When changes in albedo were translated into radiative forcing within lodgepole pine stands, radiative forcing peaked during winter, spring, summer, and annually 10 years post attack and in fall 11 years post attack ($-1.7 \pm 0.2 \text{ W m}^{-2}$, $-0.5 \pm 0.1 \text{ W m}^{-2}$, and $0.03 \pm 0.004 \text{ W m}^{-2}$, $-0.6 \pm 0.1 \text{ W m}^{-2}$, and $-0.3 \pm 0.04 \text{ W m}^{-2}$, respectively) (Figure 5). Within ponderosa pine stands, meanwhile, radiative forcing peaked during winter, spring, summer, and annually 10 years post attack and in fall 3 years post attack ($-1.4 \pm 0.2 \text{ W m}^{-2}$, $-0.3 \pm 0.03 \text{ W m}^{-2}$, and $0.05 \pm 0.006 \text{ W m}^{-2}$, $-0.5 \pm 0.06 \text{ W m}^{-2}$, and $-0.5 \pm 0.07 \text{ W m}^{-2}$, respectively) (Figure 6).

At a monthly timescale, radiative forcing peaked for both lodgepole pine and ponderosa pine in January 10 years post attack at $-2.1 \pm 0.4 \text{ W m}^{-2}$ and $-1.7 \pm 0.4 \text{ W m}^{-2}$, respectively.

[20] By incorporating the total area of attack in each year (1994–2011) (Figure 1) and the radiative forcing for a given location based on years since the attack started (Figures 5 and 6), we quantified the per year radiative forcing in megawatts for mountain pine beetle attacked lodgepole pine and ponderosa pine forests. Annual radiative forcing showed an exponential increase over the time period from -1.9 MW

in 1997 to -380.9 MW in 2011 (Figure 7). Most of the annual radiative forcing occurred during the winter months. In 2011 the rate of radiative forcing reached -982.7 ± 139.0 MW, -269.8 ± 38.2 MW, -31.1 ± 4.4 MW, and -147.8 ± 20.9 MW in winter, spring, summer, and fall, respectively (Figure 7). The global climate impact of mountain pine beetle outbreaks within our study area and time period was then quantified by dividing the rate of radiative forcing (Watts) by the surface of the Earth. The cumulative (1994–2011) annual albedo feedback, due to mountain pine beetle outbreaks within the study area, created a radiative forcing of $-3.5 \times 10^{-6} \text{ W m}^{-2}$ when normalized over the entire Earth surface. Although this number is very small, the area of mountain pine beetle impacted forest within the study area represents only $\sim 2\%$ of the current bark beetle epidemic spread across North America, with 19.4 million ha and 16.9 million ha across western Canada and western U.S., respectively, and additional attacks occurring in Eurasia [USDA Forest Service, 2011].

[21] Finally, we assessed the spatial variability of the cumulative radiative forcing within the study area, driven by forest type, monthly change in albedo, and years since the outbreak started. Radiative forcing ranged from -0.2 to -13.1 MJ m^{-2} (Figure 8). Cumulative radiative cooling was highest in the Vasquez Mountains west of Winter Park and the Black Forest northeast of Colorado Springs. Cumulative radiative cooling was also high in the Rabbit Ear Range west of Grand Lake, the Williams Fork Mountains west of Winter Park, the Grand Lake area, and the northwest portion of the Park Range north of Steamboat Springs (Figure 8). Cumulative radiative cooling was lowest in ponderosa pine stands on the eastern side of the Front Range (Figure 8).

4. Discussion

[22] The observed increase in both lodgepole pine and ponderosa pine winter albedos in response to mountain pine beetle damage was likely due to the increased above-canopy visibility of snow associated with tree mortality (needle loss and snag fall). This finding is consistent with model-derived deforestation impacts as well as site-level bark beetle impacts reported by others [Betts, 2000; Bala et al., 2007; O'Halloran et al., 2012]. Several studies have documented a decrease in below-canopy winter albedo in the first several years following an attack due to needle deposition on snow [Pugh and Small, 2012; Winkler et al., 2010]. With adequate mortality and the loss of overstory vegetation, we might expect that this needle deposition could impact above-canopy albedo as well. We did not find a significant decrease in above-canopy albedo following the attack; instead, both forest types exhibited a 3 year lag effect before a significant increase in winter albedo was seen ($p < 0.05$), presumably correlating with the needlefall period. During the growing season, a change to summer albedo could be expected in response to increased exposure of bright, dry soil and understory vegetation. Both lodgepole pine and ponderosa pine forest types showed a consistent but modest and largely nonsignificant increase in summer and fall albedos in response to mountain pine beetle attack. It is interesting to note, however, that both O'Halloran et al. [2012] and Maness et al. [2013] also documented a small increase in summer albedo, suggesting

that this change, although small, may represent a shift in vegetation dynamics in response to mountain pine beetle outbreaks. In regard to the role of forest type, both the lodgepole pine and ponderosa pine forests showed similar seasonal responses to mountain pine beetle outbreaks; however, lodgepole pine stands showed significantly higher changes to winter and spring albedos in several years, relative to ponderosa pine stands. This difference could be attributed to species-based differences in stand density and outbreak severity. It could also be attributed to the spatial distribution of lodgepole pine versus ponderosa pine stands. Lodgepole pine stands tend to be found at higher elevations than ponderosa pine stands [Cochran and Berntsen, 1973], where snow can be expected to be more consistent and persist longer in the winter and spring months. As snow cover is a key driver to large changes in albedo, the elevational distribution of these stands could also explain species-related differences.

[23] One unexpected finding in the analysis was a decrease in lodgepole pine and ponderosa pine albedos at 12 to 15 years post outbreak. Such a pattern could have either an ecological or sampling explanation. O'Halloran et al. [2012] observed a similar decrease and argued that temporary decreases in albedo post outbreak may be related to the rapid growth of surviving and understory trees, associated with increased resource availability post outbreak [Cole and Amman, 1980; Greene et al., 1999]. They further argued that an increase in albedo could be expected 15 years after attack with snag fall. Alternatively, as the outbreak in the region began in the mid to late 1990s, the finding could be a scale-related anomaly resulting from the upscaling of a patchy outbreak to MODIS resolution, which could have resulted in a lower mean severity for older outbreaks.

[24] Our observed change in winter albedo due to mountain pine beetle outbreaks (maximum mean increase of 0.06 ± 0.01 and 0.05 ± 0.01 10 years post outbreak in lodgepole pine and ponderosa pine stands, respectively) was much smaller than that documented by others due to changes in land cover. Barnes and Roy [2010] documented a snow albedo change of 0.19 and 0.21 from forest to nonmechanically disturbed and grassland/shrubland, respectively using MODIS shortwave white-sky albedo. Jin et al. [2002] used MODIS shortwave black-sky snow albedo and documented a change of 0.08 and 0.24 from evergreen needleleaf forest to deciduous broadleaf forest and open shrub, respectively. In contrast, Betts [2000] documented a change of 0.52 in snow albedo from dense coniferous forest to arable cropland. One caveat in these comparisons is that unlike the studies described above, our analysis did not restrict winter albedo to snow-covered conditions (both snow-covered and snow-free areas were included), thus lowering the winter albedo change we reported.

[25] We can also compare our radiative forcing findings with other disturbance-related studies. The order of magnitude of local radiative forcing observed in our study within bark beetle damaged areas was similar to that found by O'Halloran et al. [2012] (peak albedo radiative forcing of $-2.4 \pm 0.4 \text{ W m}^{-2}$ at 11 years post mountain pine beetle attack). Additionally, the radiative forcing of mountain pine beetle attacks can be compared to the impact of forest fires, another disturbance type common to the south-central Rocky Mountains. At a site scale the magnitude of radiative forcing for both ponderosa pine and lodgepole pine

mountain pine beetle outbreaks (annual average (3–15 years) $= -0.3 \pm 0.04 \text{ W m}^{-2}$) was less than that observed by *Randerson et al.* [2006] post-fire ($-5 \pm 2 \text{ W m}^{-2}$ for year 1 and $-4.2 \pm 2.0 \text{ W m}^{-2}$ for years 0 to 80). It should be noted that the albedo change reported by *Randerson et al.* [2006] was derived from a single-fire event, whereas our results report an annual mean across a range of outbreak severities and site conditions. The smaller radiative cooling from mountain pine beetle outbreaks may be somewhat compensated by the larger spatial extent of mountain pine beetle outbreaks relative to fire within Colorado and southern Wyoming over the same time frame. Fire extent (as derived from MTBS data) was 396,800 ha for 1994–2010 compared to 1,322,700 ha of mountain pine beetle outbreak (1994–2010) within lodgepole and ponderosa pine forests.

[26] The next step in quantifying the full albedo-related radiative forcing effect due to mountain pine beetle outbreaks will require the application of albedo trajectories into the future to account for lagged and persisting effects. In a separate study we have used plot-based data from historical to present outbreaks in order to extend these albedo trajectories and determine the historical effect of mountain pine beetle outbreaks on radiative forcing [*Vanderhoof et al.*, 2013]. Additionally, although this work extends previous site-level studies and attempts to document the landscape-scale effects of bark beetles, our study area still represents only ~2% of the current epidemic's North America bark beetle affected forest. Future work is needed to quantify the radiative forcing of mountain pine beetle outbreaks across the western United States. It is important to note that the cumulative radiative forcing due to mountain pine beetle outbreaks can be expected to be regionally specific due to climate-induced differences in tree growth and regional differences in mountain pine beetle outbreak dynamics and host tree spatial abundance.

[27] A full radiative forcing analysis for mountain pine beetle outbreaks must also consider committed carbon emissions or the expected future CO_2 emissions associated with the decomposition of beetle-killed trees (B. Ghimire et al., Large carbon release from bark beetle outbreaks across western United States imposes climate feedback, submitted to *Global Change Biology*, 2013). However, while the albedo radiative forcing component will occur immediately, as will a reduction in net ecosystem carbon uptake due to a stand reduction in leaf area index and associated productivity, a substantial lag will occur before killed trees fully decompose (the committed CO_2 emissions). Snags begin to fall 5 years after stand death, with blowdown peaking in 10–15 years [*Mitchell and Preisler*, 1998]. Decomposition is typically very limited in standing snags [*Naesset*, 1999; *Mäkinen et al.*, 2006]. More importantly, the turnover time for lodgepole pine coarse woody debris in the Colorado Rocky Mountains can be on the order of hundreds of years, ranging from 340 ± 130 years to 630 ± 410 years depending on temperature [*Brown et al.*, 1998; *Kueppers et al.*, 2004]. This time lag between albedo and carbon radiative forcing is important to recognize.

[28] Lastly, we note that bark beetle outbreaks have potential consequences for the hydrological cycle as well. Reductions in summer evapotranspiration post outbreak [*Mikkelsen et al.*, 2013; *Maness et al.*, 2013] could result in a positive feedback mechanism, in which a reduction in summer evapotranspiration results in reduced precipitation and increased drought conditions which may exacerbate

current outbreaks that are stimulated by warmer, drier conditions. Alternatively, the documented decrease in a winter radiative forcing, due to the transition from a dark tree-covered surface to a light snow-covered surface could result in cooler wintertime air temperatures, potentially reducing beetle populations because of winter “cold snaps” known to kill beetles. The direction and balance of these two mechanisms, temperature and precipitation feedbacks, will likely contribute to the persistence or reduction of mountain pine beetle outbreaks across the Rocky Mountains over the next decade and beyond.

5. Conclusions

[29] Mountain pine beetle attacks progress across landscapes over years to decades, which means that although individual sites may start to recover, damage can accumulate across the landscape, necessitating a landscape-scale analysis. The purpose of this study was to observe if the pattern of albedo change, observed by others at a site scale, persisted when averaged across large, variable areas of outbreak, and how site-specific radiative forcing translated to regional radiative forcing. Although change is spatially variable, as observed in Figure 1, changes in albedo with years since outbreak start, as shown in Figures 2 and 3, demonstrate that general patterns of change in albedo with season and time since disturbance persist when we use landscape-scale data sets (i.e., MODIS and USFS ADS) despite potential contamination from data set error, variable stand density, outbreak severity, and undocumented, unrelated sources of disturbance (e.g., harvest events and small fires). Our work also demonstrated exponential growth in winter and annual radiative forcings over time across the study area, due to both persistent and rising albedo effects with time since disturbance, as well as the expanding area of attacked forest. With millions of hectares of forests already affected by mountain pine beetle, this study documented an important biogeophysical effect occurring through albedo impacts.

[30] **Acknowledgments.** This work was funded by the 2011–2013 NASA Earth and Space Science Fellowship (NESSF) (11-Earth11F-134 and 12-Earth12R-59). Additional financial support was received from the NASA ROSES09 Science of Terra and Aqua program through grant NNX11AG53G. We thank Rocky Mountain National Park for their field support; Marcus Pasay for his assistance with field work; and Jefferey Masek, Crystal Schaaf, Feng Gao, and the anonymous reviewers for their insightful comments.

References

- Bala, G., K. Caldeira, M. Wickett, T. J. Phillips, D. B. Lobell, and A. Mirin (2007), Combined climate and carbon-cycle effects of large-scale deforestation, *Proc. Natl. Acad. Sci. U.S.A.*, **104**(16), 6550–6555.
- Barnes, C. A., and D. P. Roy (2008), Radiative forcing over the conterminous United States due to contemporary land cover land use albedo change, *Geophys. Res. Lett.*, **35**, L09706, doi:10.1029/2008GL033567.
- Barnes, C. A., and D. P. Roy (2010), Radiative forcing over the conterminous United States due to contemporary land cover land use change and sensitivity to snow and interannual albedo variability, *J. Geophys. Res.*, **115**, G04033, doi:10.1029/2010JG001428.
- Bentz, B., J. Logan, J. MacMahon, and C. Allen (2009), *Bark Beetle Outbreaks in Western North America: Causes and Consequences*, University of Utah Press, Chicago, IL.
- Berg, E. E., J. D. Henry, C. I. Fastie, A. D. de Volder, and S. M. Matsuoka (2006), Spruce beetle outbreaks on the Kenai Peninsula, Alaska and Kluane National Park and Reserve, Yukon Territory: Relationship to summer temperatures and regional differences in disturbance regimes, *For. Ecol. Manage.*, **227**, 219–232.
- Betts, R. A. (2000), Offset of the potential carbon sink from boreal forestation by decreases in surface albedo, *Nature*, **408**, 187–190.

- Brown, P. M., W. D. Shepperd, S. A. Mata, and D. L. McClain (1998), Longevity of windthrown logs in a subalpine forest of central Colorado, *Can. J. For. Res.*, 28, 932–936.
- Cochran, P. H., and C. M. Berntsen (1973), Tolerance of lodgepole and ponderosa pine seedlings to low night temperatures, *For. Sci.*, 19(4), 272–280.
- Cole, W. E., and G. D. Amman (1980), *Mountain Pine Beetle Dynamics in Lodgepole Pine Forests: Part 1. Course of an Infestation*, General Technical Report INT-89, U.S. Department of Agriculture Forest Service, Intermountain Research Station, Ogden, Utah.
- Collins, W. D., P. J. Rasch, B. A. Boville, J. J. Hack, J. R. McCaa, D. L. Williamson, and B. P. Briegleb (2006), The formulation and atmospheric simulation of the Community Atmosphere Model Version 3 (CAM3), *J. Clim.*, 19, 2144–2161.
- Committee on Radiative Forcing Effects on Climate, Climate Research Committee, and National Research Council (2005), *Radiative Forcing of Climate Change: Expanding the Concept and Addressing Uncertainties*, 224 pp., The National Academies Press, Washington, D. C.
- Eidsenink, J., B. Schwind, K. Brewer, Z. Zhu, B. Quayle, and S. Howard (2007), A project for monitoring trends in burn severity, *Fire Ecol.*, 3(1), 3–21.
- Gao, F., C. B. Schaaf, A. H. Strahler, A. Roesch, W. Lucht, and R. Dickinson (2005), MODIS bidirectional reflectance distribution function and albedo Climate Modeling Grid products and the variability of albedo for major global vegetation types, *J. Geophys. Res.*, 110, D01104, doi:10.1029/2004JD005190.
- Greene, D. F., J. C. Zasada, L. Sirois, D. Kneeshaw, H. Morin, I. Charron, and M. J. Simard (1999), A review of the regeneration dynamics of North American boreal forest tree species, *Can. J. For. Res.*, 29, 824–839.
- Hansen, J., M. Sato, and R. Ruedy (1997), Radiative forcing and climate response, *J. Geophys. Res.*, 102(D6), 6831–6864, doi:10.1029/96JD03436.
- Huggard, D., and D. Lewis (2007), *Effects of Salvage Options for Beetle-killed Pine Stands on ECA*, Draft Report, 41, BC Ministry of Environment, Kamloops.
- Intergovernmental Panel on Climate Change (2000), *Good Practice Guidance and Uncertainty Management in National Greenhouse Gas Inventories*, edited by J. Penman, D. Kruger and I. Galbally, 6.1–6.34, Inst. for Global Environ. Strategies, Kanagawa, Japan.
- Jin, Y., C. B. Schaaf, F. Gao, X. Li, A. H. Strahler, X. Zeng, and R. E. Dickinson (2002), How does snow impact the albedo of vegetated land surfaces as analyzed with MODIS data? *Geophys. Res. Lett.*, 29(10), 1374, doi:10.1029/2001GL014132.
- Jin, Y., C. B. Schaaf, C. E. Woodcock, F. Gao, X. Li, A. H. Strahler, W. Lucht, and S. Liang (2003), Consistency of MODIS surface bidirectional reflectance distribution function and albedo retrievals: 2. Validation, *J. Geophys. Res.*, 108(D5), 4159, doi:10.1029/2002JD002804.
- Klutsch, J. G., J. F. Negron, S. L. Costello, C. C. Rhoades, D. R. West, J. Popp, and R. Caissie (2009), Characteristics and downed woody debris accumulations associated with mountain pine beetle (*Dendroctonus ponderosae* Hopkins) outbreak in Colorado, *For. Ecol. Manage.*, 258, 641–649.
- Kueppers, L. M., J. Southon, P. Baer, and J. Harte (2004), Dead wood biomass and turnover time, measured by radiocarbon along a subalpine pine elevation gradient, *Oecologia*, 141, 641–651.
- Mäkinen, H., J. Hynynen, J. Siitonen, and R. Sievänen (2006), Predicting the decomposition of Scots pine, Norway spruce, and birch stems in Finland, *Ecol. Appl.*, 16(5), 1865–1879.
- Maness, H., P. J. Kushner, and I. Fung (2013), Summertime climate response to mountain pine beetle disturbance in British Columbia, *Nat. Geosci.*, 6, 65–70.
- Mikkelsen, K. M., R. M. Maxwell, I. Ferguson, J. D. Stednick, J. E. McCray, and J. O. Sharp (2013), Mountain pine beetle infestation impacts: Modeling water and energy budgets at the hill-slope scale, *Ecohydrology*, 6(1), 64–72.
- Mitchell, R. G., and H. K. Preisler (1998), Fall rate of lodgepole pine killed by the mountain pine beetle in central Oregon, *West J. Appl. For.*, 13(1), 23–26.
- Naesset, E. (1999), Decomposition rate constants of *Picea abies* logs in southeastern Norway, *Can. J. For. Res.*, 29(3), 372–381.
- O'Halloran, T. L., et al. (2012), Radiative forcing of natural forest disturbances, *Global Change Biol.*, 18(2), 555–565.
- Painter, T. H., K. Rittger, C. McKenzie, P. Slaughter, R. E. Davis, and J. Dozier (2009), Retrieval of subpixel snow covered area, grain size, and albedo from MODIS, *Remote Sens. Environ.*, 113, 868–879.
- Pugh, E., and E. Small (2012), The impact of pine beetle infestation on snow accumulation and melt in the headwaters of the Colorado River, *Ecohydrology*, 5(4), 467–477.
- Raffa, K. F., B. H. Aukema, B. J. Bentz, A. L. Carroll, J. A. Hicke, M. G. Turner, and W. H. Romme (2008), Cross-scale drivers of natural disturbances prone to anthropogenic amplification: The dynamics of bark beetle eruptions, *BioScience*, 58, 501–517.
- Randerson, J. T., et al. (2006), The impact of boreal forest fire on climate warming, *Science*, 314, 1130–1132.
- Roman, M. O., et al. (2009), The MODIS (Collection V005) BRDF/albedo product: assessment of spatial representativeness over forested landscapes, *Remote Sens. Environ.*, 113, 2476–2498.
- Ruefenacht, B., et al. (2008), Conterminous U.S. and Alaska forest type map ponderosa pines using forest inventory and analysis data, *Photogramm. Eng. Remote Sens.*, 74(11), 1379–1388.
- Schaaf, C. B., et al. (2002), First operational BRDF, albedo nadir reflectance products from MODIS, *Remote Sens. Environ.*, 83, 135–148.
- Shell, K. M., J. T. Kiehl, and C. A. Shields (2008), Using the radiative kernel technique to calculate climate feedbacks in NCAR's Community Atmospheric Model, *J. Clim.*, 21, 2269–2282.
- USDA Forest Service (2011), Western bark beetle strategy. USDA Forest Service.
- Vanderhoof, M., C. A. Williams, Y. Shuai, D. Jarvis, D. Kulakowski, and J. Masek (2013), Albedo-induced radiative forcing from mountain pine beetle outbreaks in forests, south-central Rocky Mountains: Magnitude, persistence, and relation to outbreak severity, *Biogeosciences Discuss.*, 10, 1–34.
- Wang, K., S. Liang, C. L. Schaaf, and A. H. Strahler (2010), Evaluation of Moderate Resolution Imaging Spectroradiometer land surface visible and shortwave albedo products at FLUXNET sites, *J. Geophys. Res.*, 115, D17107, doi:10.1029/2009JD013101.
- Winkler, R., S. Boon, B. Zimonick, and K. Baleshta (2010), Assessing the effects of post-pine beetle forest litter on snow albedo, *Hydrol. Processes*, 24(6), 803–812.
- Zhang, Y. C., W. B. Rossow, and A. A. Lacis (1995), Calculation of surface and top of atmosphere radiative fluxes from physical quantities based on ISCCP data sets: 1. Method and sensitivity to input data uncertainties, *J. Geophys. Res.*, 100(D1), 1149–1165.